



HAL
open science

Theoretical investigations of a highly mismatched interface: the case of SiC/Si(001)

Laurent Pizzagalli, Giancarlo Cicero, Alessandra Catellani

► To cite this version:

Laurent Pizzagalli, Giancarlo Cicero, Alessandra Catellani. Theoretical investigations of a highly mismatched interface: the case of SiC/Si(001). *Physical Review B: Condensed Matter and Materials Physics* (1998-2015), 2003, 68 (19), pp.195302. <10.1103/PhysRevB.68.195302>. <hal-00171004>

HAL Id: hal-00171004

<https://hal.science/hal-00171004v1>

Submitted on 11 Sep 2007

HAL is a multi-disciplinary open access archive for the deposit and dissemination of scientific research documents, whether they are published or not. The documents may come from teaching and research institutions in France or abroad, or from public or private research centers.

L'archive ouverte pluridisciplinaire **HAL**, est destinée au dépôt et à la diffusion de documents scientifiques de niveau recherche, publiés ou non, émanant des établissements d'enseignement et de recherche français ou étrangers, des laboratoires publics ou privés.



HAL Authorization

Theoretical investigations of a highly mismatched interface: the case of SiC/Si(001)

Laurent Pizzagalli*

*Laboratoire de Métallurgie Physique, UMR 6630, CNRS & Université de Poitiers,
BP 30179, F-86962 Futuroscope Chasseneuil Cedex, France*

Giancarlo Cicero

*CNR-IMEM, Parco Area delle Scienze, 37A, I-43010 Parma, Italy; and INFN and Physics Department,
Polytechnic of Torino, C.Duca degli Abruzzi, 24, I-10129 Torino, Italy*

Alessandra Catellani

CNR-IMEM, Parco Area delle Scienze, 37A, I-43010 Parma, Italy

(Dated: September 11, 2007)

Using first principles, classical potentials and elasticity theory, we investigated the structure of a semiconductor/semiconductor interface with a high lattice mismatch, SiC/Si(001). Among several tested possible configurations, a heterostructure with (i) a misfit dislocation network pinned at the interface and (ii) reconstructed dislocation cores with a carbon sub-stoichiometry is found to be the most stable one. The importance of the slab approximation in first principles calculations is discussed and estimated by combining classical potential techniques and elasticity theory. For the most stable configuration, an estimate of the interface energy is given. Finally, the electronic structure is investigated and discussed in relation with the dislocation array structure. Interface states, localized in the heterostructure gap and located on dislocation cores, are identified.

PACS numbers: 68.35-p, 81.05.Hd, 81.15.Aa

I. INTRODUCTION

The misfit strain present in lattice mismatched epitaxial layers has been widely studied because of its omnipresence in the heterostructures used in device technology. Two goals are usually pursued, either to avoid strain for preparing long-lived devices, or to exploit the modified electronic properties of strained layers for obtaining specific devices such as lasers.^{1,2} The general picture of heteroepitaxy is well known. First, strained layers are grown on the substrate. Over a critical thickness, which depends on the elastic properties and the lattice mismatch between the two materials, plastic relaxation of the strain with formation of misfit dislocations becomes energetically favorable. In the case of small mismatch, the critical thickness can be large, with a low dislocation density. For example, a critical thickness of about 10^3 Å is measured for a lattice mismatch of 1% in $\text{Ge}_x\text{Si}_{1-x}$ layers ($x = 0.24$)³, and the average separation between misfit edge dislocations is estimated to be about 390 Å (for [001] layers). Each dislocation is far from the others and from the interface, and the system can be described by considering an ideal coherent interface, with strained layers. Hoekstra and Kohyama used this frame for investigating the β -SiC(001)/Al interface.⁴ In a scheme recently proposed, Benedek *et al.* introduced an additional correction for the effect of the misfit dislocations⁵, by comparing coherent and semi-coherent interfaces. However, in the case of heteroepitaxy for largely mismatched systems, the critical thickness is very low and a dense network of misfit dislocations is present in the grown layers. The interactions between dislocations and between the interface and the dislocations must then be explicitly

taken into account.

Despite the large lattice mismatch of $\sim 20\%$, β -SiC can be grown on Si(001), using different techniques.^{6,7,8,9} A recent High-Resolution Electron Microscopy (HREM) study of this system shows a locally abrupt interface, with the presence of a periodic array of misfit dislocations.^{7,8,9} These ones seem to be located directly at the interface, which points at a vanishing critical thickness for this heterostructure. It is difficult to gain additional information from these experiments. In particular, the atomic structure and the chemical environment at the interface, which deeply affect its physical properties, still remain hardly accessible. Atomistic computations are a possible solution for complementing the experiments. In addition, first principle calculations would allow the determination of the electronic properties of the heterostructure. In this respect, the SiC/Si interface may be considered as a model for a high lattice mismatch interface between covalent materials, just as silicon is usually considered as the semiconductor prototype. Indeed, due to the peculiar lattice mismatch, almost equal to 20%, the network dislocation pattern is extremely dense and can be modelled within a cell small enough to make an ab initio computation affordable.

As far as we know, few studies have been devoted to the SiC/Si(001) system. Chirita *et al.*¹⁰ have investigated the strain relaxation and the thermal stability of the interface using the semi-empirical classical potential from Tersoff.¹¹ They have obtained a possible configuration of the atomic structure, stable up to 1000 K. However, they assumed a stoichiometric interface, which may be a metastable state. Another study from Kitabatake with the same potential choice was exclusively focussed

on the first step of the formation of the interface, *i.e.* a pre-carbonization of the Si(001) surface prior to growth.⁹ A detailed investigation of the atomic structure and stoichiometry of the SiC/Si(001) interface with first principle techniques is still lacking. The large computational cell required for the modelling, notwithstanding the advantageous lattice mismatch, may explain the absence of such calculations.

Recently, we have presented in a letter the most striking results of the first ab initio study of the SiC/Si(001) interface.¹² Here, we provide a thorough description of our investigations, combining elasticity theory, classical potentials and first principles calculations. In particular, after a complete explanation of the computational procedure, the full set of tested atomic configurations is presented. We have investigated the stoichiometry of the interface as well as its stability with few pseudomorphic SiC layers. The determination of the interface energy as well as the analysis of finite size effects in the slab approximation are also presented. Finally, the computed electronic structure of the most stable configuration is discussed.

II. COMPUTATIONAL PROCEDURE

A. Model

Considering that the lattice parameters of Si and 3C-SiC are respectively $a(\text{Si}) = 5.4309 \text{ \AA}$ and $a(\text{SiC}) = 4.3596 \text{ \AA}$ ¹³, the calculated misfit $(a(\text{Si}) - a(\text{SiC}))/a(\text{Si})$ at the interface is 19.73%. Within the hypothesis of a coherent interface, such a misfit is equivalent to a huge tensile stress in the SiC layers. A simple estimate shows that the elastic energy stored in the coherent film would be approximately $1.6 \text{ J/m}^2/\text{layer}$.¹⁴ However, it is observed that the interface is semi-coherent, the stress being relaxed by the introduction of a network of undissociated edge dislocations of Burgers vector $b = a(\text{SiC})/2\langle 110 \rangle$, with dislocation lines lying along the $[110]$ and $[\bar{1}10]$ directions.^{7,8,9} Due to the peculiar value of the misfit, approximately equal to $\frac{1}{5}$, the semi-coherence is obtained when the spacing between misfit dislocations is $5b$. The SiC/Si(001) interface is then modelled by matching a $p(5 \times 5)$ -SiC(001) slab (N layers) with a $p(4 \times 4)$ -Si(001) slab (M layers) along the $[001]$ direction (z-axis), at the Si lattice parameter, optimized for bulk calculations with the chosen method. In the following, size conditions for a system will be simply designed by N/M. Periodic boundary conditions are applied along $[110]$ and $[\bar{1}10]$ directions (x- and y-axis) in any case. Atoms belonging to the topmost SiC and bottommost Si layers were fixed in bulk positions. However, in order to better relax the interface, the SiC topmost layer was allowed to move as a whole in all directions. This procedure was achieved at each step by (i) compute the average of atomic forces in this layer, (ii) apply this force to all layer atoms. Once the structures were converged, we also performed additional

calculations to check the effect of the surfaces on the interface by releasing the constraints on both surfaces.

B. Methods

Classical molecular dynamics calculations were done with the semi-empirical Tersoff potentials¹¹, at the lattice parameter $a(\text{Si}) = 5.43 \text{ \AA}$. This choice is currently the best available for describing solid SiC. A recent study has revealed that it reproduces DFT results on the formation energies and properties of native defects in SiC with a good accuracy.¹⁵ Here, several system sizes were considered, because of the low CPU time and memory requirements for these calculations. The exploration of the configurational space was typically done with 12/8 and 36/36 slabs, to ensure that the interaction between the interface and the surfaces is negligible. To estimate this interaction, sizes as large as 50/50 have been considered.

First principles calculations were performed¹⁶ within the Density Functional Theory (DFT), in the Local Density Approximation (LDA).¹⁷ An energy cutoff of 40 (160) Ry was used for the plane waves expansion of the wavefunctions (charge density). The reciprocal space integration in the supercell Brillouin Zone (BZ) was done by considering only the Γ point. The core electrons were removed by using pseudopotentials, with *s* and *p* non-locality for Si and *s* non-locality for C.¹⁸ We used a calculated Si lattice parameter of 5.401 \AA , consistent with our ab initio pseudopotential. Surface atoms at both sides were saturated with hydrogens. The C-H and Si-H distances were optimized independently by fully relaxing surface saturated symmetric slabs of 11 layers, 8 atoms each. 5/5 and 7/7 system sizes were used, which corresponds to large scale calculations with at most 369 atoms. At variance with classical simulations, periodic boundary conditions were also applied along the $[001]$ direction, a large vacuum space (9.1 \AA for 5/5, 8.2 \AA for 7/7) being introduced to prevent spurious surface-surface interactions. All structures were considered converged when forces acting on atoms were less than 10^{-4} a.u. (0.005 eV/\AA) and energy varied by less than 10^{-5} eV/atom.

C. Configuration energy

In this work, we have always compared the energies of systems with the same N/M. The numbers of C and Si atoms in the SiC slab may however change for two N/M slabs with different interface configurations. In addition, the surface of the SiC slab may be either Si- or C-terminated. Hence, the energy E_{slab} of the N/M slab model described above, obtained from either methods, cannot be used directly for determining the most stable structure. Instead, a configuration energy E_{α} , given by the following expression, can be defined within the grand canonical frame:

III. STABILITY AND GEOMETRY

$$E_\alpha = E_{slab} - E_S^{\text{SiC}} - E_S^{\text{Si}} - n^{\text{Si}} \mu^{\text{Si}} - n^{\text{C}} \mu^{\text{C}} \quad (1)$$

E_S^{SiC} is the surface energy of the SiC part of the slab, Si- or C-terminated depending on the configuration at the interface and on the number of layers, whereas E_S^{Si} is the surface energy of the Si part. n^{Si} and n^{C} are the numbers of Si or C atoms in the SiC/Si slab. Finally, μ^{Si} and μ^{C} are the chemical potentials for each species. For the Si part of the slab, μ^{Si} is equal to the bulk silicon chemical potential. Though μ^{Si} and μ^{C} cannot be exactly determined for the SiC part, it is possible to determine a range of thermodynamically allowed values.¹⁹ The following relations must be satisfied at the same time:

$$\mu^{\text{Si}} + \mu^{\text{C}} = \mu_0^{\text{SiC}} \quad (2)$$

$$\mu_0^{\text{Si}} + \mu_0^{\text{C}} - \Delta\mathcal{H}_f = \mu_0^{\text{SiC}} \quad (3)$$

Here, the μ_0^I are the chemical potentials of the mono-elemental bulk phases, and are easily calculated. $\Delta\mathcal{H}_f$ is the heat of formation of silicon carbide: in this work, we used the experimental value, $\Delta\mathcal{H}_f = 0.72$ eV. These two relations reveal that the Si and C chemical potential values are linked, and that the chemical potential of one species is always equal or lower than the chemical potential of the mono-elemental bulk phase. The allowed ranges are then

$$\mu^{\text{Si}} \in [\mu_0^{\text{Si}} - \Delta\mathcal{H}_f, \mu_0^{\text{Si}}] \quad (4)$$

$$\mu^{\text{C}} \in [\mu_0^{\text{C}} - \Delta\mathcal{H}_f, \mu_0^{\text{C}}] \quad (5)$$

$(\mu_0^{\text{Si}} - \Delta\mathcal{H}_f, \mu_0^{\text{C}})$ corresponds to C-rich (Si-poor) conditions and $(\mu_0^{\text{Si}}, \mu_0^{\text{C}} - \Delta\mathcal{H}_f)$ to C-poor (Si-rich) conditions. The values obtained in the present work for μ_0^I are listed in Table I: here, for the ab initio results, we indicate the respective values as obtained from standard converged bulk calculations and as extrapolated from surface calculations with the scheme originally proposed by Fiorentini and Methfessel.²⁰ This will be useful to determine the different contributions in Eqn. (1) and the interface energy, as described below. It is worth noting that extreme caution must be adopted when estimating μ_0^I , as small ($\simeq 1\%$) errors in this quantity are then multiplied by the usually large number of atoms at the interface, eventually producing non-physical results. The use of the linearized values of μ_0^I in this work yields different configuration energy values with respect to our previously published results¹², without changing the original qualitative conclusions.

Using the configuration energies allows to compare interface structures in the slab approximation, with different surface terminations and number of atoms. In the following, we discuss the stability of different configurations.

In a previous work on the SiC/Si(001) interface, Chirita *et al.* proposed a possible geometry of the interface¹⁰, based on molecular dynamics calculations. In the choice of their initial atomic configuration, they have made several hypothesis. They assumed that the dislocations network is pinned directly at the interface, that the first (001) layer of the SiC slab is silicon-like, and finally, that the interface remains perfectly stoichiometric. However, from HREM experiments, it is hard to extract such information. An interface with a pseudomorphic first layer followed by a misfit dislocations network is possible, as well as reconstructed misfit dislocation cores including a sub- or over-stoichiometry in carbon and/or silicon atoms. In our work, we have taken into account such possibilities, and our search for the most stable configuration has been broadened by considering a large set of initial geometries, by means of classical molecular dynamics. First, only interfaces made with complete layers were investigated. Fig. 1 shows 6 different possible starting geometries. The first ones, S1 and S2, are stoichiometric configurations with the misfit dislocation array located directly at the interface. In S1, the first SiC layer is carbon-like whereas it is silicon-like in S2 (S2 is the initial configuration selected in the previous study¹⁰). In P1 and P2, the misfit dislocation array is located in the second and third SiC layers, respectively. Those are obtained by removing one or two $p(5\times 5)$ SiC layers, replaced by $p(4\times 4)$ pseudomorphic layers. Finally, we also compared the previous structures with configurations C1 and C2, with a higher carbon concentration at the interface (carbonization).

The configuration energy differences are reported in Table II. Here, the calculated values are easily extracted from the classical dynamics, as the energy of each atom is a well defined quantity in the interaction potential model. The S2 configuration, investigated in a previous study¹⁰, is stable but is clearly not the lowest energy solution. Instead, the most stable structures are obtained for a stoichiometric system and a C layer at the interface, i.e. S1. For such structures, we found two different atomic configurations, represented in Fig. 2. It must be emphasized that the two [110] and $[1\bar{1}0]$ directions, perpendicular to the interface, are not equivalent due to the peculiar zincblende stacking. The first configuration, called S1a, has the lowest energy in the full range of chemical potentials. Along [110], bonds are formed between the extra C atoms located at the misfit dislocation core and Si atoms belonging to the second layer of the Si(001) slab. All these atoms are shifted toward the interface inducing large strains, especially in the softer silicon slab. Some of the Si atoms appear to be overcoordinated. Along $[1\bar{1}0]$, the main feature is a soft dimerization of the C atoms of the first SiC layer, on both sides of the misfit dislocation line. The C-C distance is shortened to 1.65-1.80 Å which allows a reduction of the number of dangling bonds (DB). This interface reconstruction is nearly similar to

the model presented by Long *et al.*⁸ The second configuration, S1b, has a higher configuration energy, with 6.55 eV in excess. The main difference with S1a concerns the [110] side. Here, no bonds are formed between the C atoms in the first SiC layer and the second layer of the silicon slab. Instead, the number of DBs belonging to C atoms is reduced by a stronger carbon dimerization along the [110] direction (clearly visible on the $[1\bar{1}0]$ view), where the C-C distance is reduced to 1.44-1.47 Å. From Table II, it seems that the occurrence of pseudomorphic SiC layers before the introduction of misfit dislocations is not favored, although the P1 structure, with one pseudomorphic layer, is the third best solution. The segregation of carbon at the interface, tested with two configurations C1 and C2, is associated with very high configuration energies. This is consistent with the general observation that the deposition of carbon on Si(001) surface does not lead to stable carbon layers but rather to the formation of silicon carbide by carbonization, the substrate supplying the Si atoms.⁹

Several information may be obtained from our results. First, one or several complete pseudomorphic SiC layers are not favorable structures, which tends to indicate that the misfit dislocation network is located at the interface and no finite critical thickness can be defined. Secondly, all the favored configurations include a carbon layer at the interface. This can be explained by the energy gained in the formation of SiC bonds, and the smaller carbon atomic radius with respect to silicon. Finally, we observed that the minimization of the configuration energy is best realized by the reduction of DBs, especially those associated to carbon atoms. However, this DB saturation occurs via the formation of bonds between initially remote atoms, and the shortening of their separation generates energetically expensive strain in the atomic structure. This is particularly true for the shortest and strongest carbon-carbon or silicon-carbon bonds.

For the lowest energy configurations, S1a and S1b, the carbon atoms, located in the first SiC layer and in the vicinity of the misfit dislocation cores, present the most stretched bonds. We investigated the possibility of an energy lowering by removing these atoms. We initially considered the S1b configuration. A significant energy reduction was obtained by removing successively C atoms along [110] (inside the ellipsis, in Fig. 2). The additional removing of the C-dimer row along $[1\bar{1}0]$ (the other ellipsis) leads to an even more stable configuration, represented in Fig. 3. The energy difference compared to S1a is -6.04 eV/cell (-15.40 eV/cell) in C-rich (C-poor) conditions, respectively.²¹ Starting from S1a, and removing the C-row along [110] and the C-dimer row along $[1\bar{1}0]$ as described previously, the energy was also lowered, and we obtained the same final structure. This configuration, which we called CSS for Carbon SubStoichiometric, shows remarkable features. Along the [110] direction, dangling bonds created by the removal of C atoms are eliminated with the formation of Si dimers 2.48-2.54 Å long. Compared to S1a, the Si atoms of the

silicon slab, previously bonded to C atoms, recover bulk-like positions, thus minimizing the strain. Along $[1\bar{1}0]$, after the removal of the C-dimer row, the core of the misfit dislocation is made of 8-atoms rings, including seven Si atoms and a lone C atom. Almost all these atoms are fully coordinated, at the expenses of some bond stretching, particularly on the Si atoms in the second layer of the SiC slab, and at the intersection of the two perpendicular dislocations. The Si-Si bonds range from 2.33 to 2.62 Å. We found that CSS is the most stable configuration using the Tersoff potential. Indeed, tests performed on structures with further C removal, or selected C/Si exchanges, brought no additional energy reduction.

The Tersoff potential results were confirmed by the ab initio method. Owing to the huge computational effort required to deal with the interface, our investigations were restricted to three configurations, *i.e.* the low energy stoichiometric S1a and S1b, and the most stable geometry CSS. First, we found that only S1a and CSS were stable, S1b relaxing spontaneously to S1a. It is known that classical potentials tend to stabilize a larger number of metastable structures compared to first principles methods.^{22,23} No major geometrical changes were found for both configurations relaxed with first principles, compared to the classical results. A better description of the atomic structure of the reconstructed dislocation cores was however obtained. Considering CSS and the [110] direction, the Si dimer lengths range between 2.42 and 2.50 Å. Along $[1\bar{1}0]$, the dislocation core is made of Si bonds 2.36-2.52 Å long. Thus the ab initio relaxation yields a more compact 8-atom ring. The energy differences between S1a and CSS are reported in Table III, for both methods and different slab lengths. Despite the small sizes imposed by ab initio simulations, it appears that the energy difference is already well converged for a 5/5 slab, with a 0.2 eV/cell variation between 5/5 and 7/7. The ab initio calculation validates our primary results, *i.e.* the CSS configuration is the most stable one, for the whole allowed range of the chemical potentials. Moreover, even in C-rich conditions, the energy difference between the two geometries is much larger than the error associated with such computations.

The analysis of the CSS configuration topology gives some hints for understanding this result. The first set of calculations has indeed shown that it is preferable to have C atoms at the interface in the first SiC layer. From the second set, it appears that misfit dislocation cores with only silicon atoms are favored, the stretching of carbon bonds being energetically expensive. In CSS, the first SiC layer is carbon-like, but there is only one C atom involved in the reconstructed dislocation cores. It also presents the peculiar characteristics that almost no atoms are sub- or over-coordinated, owing to the formation of a topological ring along one direction and the formation of a silicon dimer along the other. The CSS configuration is then the best candidate to represent the atomic structure of the SiC/Si(001) interface.

A qualitative indication of the residual strain distribu-

tion at the interface can be obtained by inspection of the deformation of the converged system coordinates, with respect to the ideal bulk-like positions. In Fig. 4, we report the layer puckering defined as the maximum deviation in the direction perpendicular to the interface, as obtained from ab initio calculations for a 7/7 system: the major deformations are localized in Si, which has smaller elastic constants than SiC. The warping decreases when moving aside the interface, in agreement with experimental results²⁴ on the structural characterization of SiC films grown on a Si(001) substrate, which evidenced an internal roughness of individual SiC planes that diminishes away from the silicon substrate. Fig. 5 represents a comparison of the residual strain field at the interface for both the CSS and S1a geometries, evaluated in terms of atomic displacements from ideal bulk-like positions. The superior efficiency of CSS in relieving the strain is clearly evidenced by simple inspection.

Regarding the critical thickness, it is interesting to compare the CSS and P1 configurations. Indeed, the SiC film in the CSS geometry is constituted by a substoichiometric C layer, as if obtained from P1 by removing four C atoms in a row. It is thus difficult to define precisely a finite critical thickness for this interface, characterized by largely reconstructed dislocation cores, although our results support the experimental findings of a dislocation network pinned at the interface.⁸

IV. EFFECT OF SLAB SIZE

The large lattice misfit between β -SiC and Si allows the investigation of the (001) interface with ab initio methods, the spacing between dislocations being about $a(\text{SiC})/2\langle 110 \rangle \simeq 15.4 \text{ \AA}$. There are only 4 (Si portion) or 5 (SiC part) atoms per $\langle 110 \rangle$ edge. However, because the problem is two-dimensional, a slab layer includes 16 (Si part) or 25 (SiC part) atoms. Computationally, the number of layers one can use to model the interface is then severely limited. Here, we managed to calculate at most a 7/7 interface, *i.e.* $\simeq 300$ atoms. Such size is enough when considering a coherent interface. Here, the presence of a periodic network of misfit edge dislocations at the interface induces a strain field in both the SiC and Si portions of the slab. It is usually assumed that the strain field penetrates each part by a distance of the order of the dislocation spacing.⁵ In our case, we should then investigate a 14/11 slab, which is beyond the capabilities of available supercomputers. Our largest calculations performed on a 7/7 slab indeed reveal that the strain field is still not negligible at both ends of the slab: when allowing for a global relaxation, the two surfaces became slightly bent, due to residual strain, which may furthermore be different for different core structures. The flat surface constrain adopted in our simulations is a valuable approximation to perform energy comparison: this constrain however modifies the strain field of the dislocation arrays and a surface-interface interaction is present in the

system. This interaction depends on the core structure at the interface, and may affect the relative stability of the configurations.

In this part, we investigate the slab size effect by means of classical potential calculations and elasticity theory. The configuration energy, defined previously in Eqn. (1), may be written as the sum of four contributions:

$$E_{\alpha}(h) = E_a + E_c + E_{el}(h) + E_{is}(h) \quad (6)$$

Here, h is the slab size. E_a is a constant adhesive energy between Si and SiC parts; E_c is the core energy of the misfit dislocation network; E_{el} is an elastic energy due to the strain field; E_{is} is the interaction energy between surface and interface, which is zero for a slab including a large (infinite) number of layers. Only three terms depend on the slab size h . E_{el} is determined by using isotropic elasticity theory and a model of misfit dislocation arrays at the interface between a thin film of height h and an infinite substrate.²⁵ The dislocation core radius²⁶ is assumed to be equal to the Burgers vector b , *i.e.* the in-plane SiC lattice parameter $a(\text{SiC})/2\langle 110 \rangle$, in the present case. Provided that E_{el} is known for each h , E_{is} may be obtained from Eqn. 6 by calculating the configuration energy E_{α} with increasing slab size, for a chosen dislocation network. Here, the surface-interface interaction energy is determined separately for both the Si and SiC parts of the slab. We performed Tersoff potential calculations for slabs 31/n (increasing the Si part) and n/31 (increasing the SiC part), with n ranging from 5 to 31, and for both the S1a and CSS configurations.

The calculated interaction energies between surface and interface, E_{is} , are shown in Fig. 6, for both configurations, in both portions of the slab, together with the sum of these terms. The SiC contribution appears larger than the Si one, for a given number of layers. Note that the interlayer spacing for SiC is about 20% lower than for Si, and more SiC layers are needed to get an equivalent contribution from the SiC and Si parts of the slab. For example, a 10/8 slab will have SiC and Si parts of nearly identical weights on E_{is} . A larger SiC contribution is then expected for a lower number of layers. Here, the difference is important, in particular for CSS with an interaction energy almost three times larger for SiC than for Si. This could be explained by the geometry of CSS. The dislocation core along one direction is reconstructed with a ring of atoms, almost entirely located in the SiC part of the slab. The surface/interface interaction is then stronger in the SiC part.

Our results confirm that the strain field penetrates by a distance of the order of the dislocation spacing⁵, and that ideally a 14/11 slab should be used. In fact, the sum of the SiC contribution for 14 layers with the Si contribution for 11 layers is less than 0.02 eV/cell, for both solutions. Assuming that the surface/interface interaction energy is mostly elastic, it is reasonable to consider that this quantity could be fairly estimated using classical potentials. Considering the total interaction energy E_{is}

in Fig. 6, for the S1a configuration, E_{is} is 0.66 eV/cell (2.36 eV/cell) for a 7/7 (5/5) slab, while for CSS, E_{is} is 0.80 eV/cell (3.69 eV/cell) for a 7/7 (5/5) slab. In all cases, E_{is} is lower than the calculated configuration energy differences, and our previous conclusions on the stability of the CSS configuration remain valid. Moreover, since the slab size effect is stronger for CSS than for S1a, using larger slabs will further increase the stability of the CSS configuration.

V. INTERFACE ENERGY

As far as we know, there is no measured value of the SiC/Si(001) interface energy. Experimentally, it is possible to determine the bonding energy, which is related to the interface energy, from wafer bonding experiments. However, a large range of values may be obtained, depending on the kind of SiC polytypes or surface terminations.²⁷ From the theoretical point of view, no value is available. Possible explanations are either the large size of the system that have to be dealt with first principles methods, or the difficulty to extract such energy from a slab calculation. A simplified frame for obtaining the interface energy of mismatched interfaces has been proposed recently.⁵ The method however does not take into account a possible reconstruction or understoichiometry of the core of the misfit dislocations, which is mandatory for the SiC/Si(001) system, as discussed above.

In order to extract the interface energy of the CSS configuration, the energies of the surfaces on both sides of the slabs have to be known. However, with ab initio methods, only the total energy is accessible, and surface energies cannot be obtained directly. Instead, they were determined by extrapolating from slabs with an increasing number of layers, following the scheme proposed by Fiorentini and Methfessel.²⁰ Si(001)-(1×1) and C:SiC(001)-(1×1) hydrogenated surfaces were investigated, since only the carbon terminated surface was relevant for the selected configurations. In order to minimize computational errors, a large (c(4×4)) slab, with increasing thickness, from 7 up to 15 layers, was used: the extrapolated values for the chemical potentials are close to those obtained from bulk calculations for Si and SiC respectively (see Table I). To be consistent with the SiC/Si interface slab calculation, each surface atom was saturated by 2 symmetric hydrogens. As a consequence, the surface energies reported in Table IV include the energies of the pseudo-hydrogens. We found a C-H distance of 1.09 Å and a bond angle $\widehat{\text{HCH}}$ of 100.6° for the C:SiC(001)-(1×1), and a Si-H distance of 1.47 Å and a bond angle $\widehat{\text{HSiH}}$ of 101.4° for the Si(001)-(1×1). We point out that we applied constraints in order to keep a symmetric dihydride Si(001)-(1×1) surface, although the most stable configuration is canted.²⁸ We forced the symmetric geometry to quickly recover a bulk-like behavior, as required by the small slab sizes adopted in the cal-

culations, since the correct canted configuration extends deeply in inner layers.

The interface energy σ_I is obtained as the converging value of the configuration energy for large N/N slabs. In the classical case, it is easily estimated with large slabs, where the interaction between surface and interface is negligible, and all the elastic energy can be considered fully pertinent to the inner layers of the slab. In this case, we obtain $\sigma_I \simeq 22.7$ eV/cell, (*i.e.* $\sigma_I \simeq 1.6$ J/m²).

Using ab initio methods, we are limited to small slabs, 5/5 and 7/7. In principle, the determination could be done in a similar way than for surface energies, using an extrapolating technique.²⁰ However, here, the available slab sizes are too small for that purpose. In fact, both elastic and interface-surface energies considerably change between the 5/5 and the 7/7 slabs. As a consequence, a linear regression would yield misleading values for the slope and intercept constants. The extrapolating scheme could be used for slabs large enough to have constant elastic and surface-interface interaction energies, *i.e.* for N/N slabs with N greater than 14 for example. Instead, we directly calculate the interface energy for a 7/7 slab, using the chemical potentials obtained via linear extrapolation, as discussed above. We computed $\sigma_I \simeq 23.0$ (22.6) eV/cell in C-rich (C-poor) conditions. This quantity is not exactly the interface energy. Indeed, for a 7/7 slab, the surface-interface interaction is not negligible and the strain energy is still not fully converged. These contributions have been determined in the previous section: for a 7/7 slab in CSS geometry the excess surface-interface interaction is 0.8 eV/cell (see Fig. 4), and the calculated residual elastic energy between an infinite interface and a 7/7 slab is 0.2 eV/cell. The corrected interface energy is then $\sigma_I \simeq 22.4$ (22.0) eV/cell (*i.e.* 1.58 (1.55) J/m²) in C-rich (C-poor) conditions. The agreement between classical and ab initio values is surprisingly good and maybe fortuitous given the technical difficulties associated with the interface energy determination in the ab initio case, or the use of the Tersoff potential that does not include properly the electronic contributions.

We wish to stress again at this point that the ab initio values provided for the interface energy are mere estimates, as small variations in *e.g.* the chemical potentials can induce large errors and even non-physical negative interface energies. Our choice in presenting these results has been to keep consistency between the chemical potentials used to eliminate the surface and bulk contributions: for this reason, we always adopted the values for μ_0^I as obtained in the linear extrapolation scheme²⁰, for large supercells, that allowed a good k_{\parallel} sampling.

VI. ELECTRONIC PROPERTIES

We now move to the description of the electronic structure of the mismatched heterostructure. The interface configuration determines the electronic properties of the system: the presence of defects such as misfit disloca-

tions can induce interface states in the band gap, that may severely modify device performances. Indeed, our results indicate that a number of interface derived states lay in the forbidden energy gap for the most stable dislocation network, although the number of DBs is in this case minimized.

For a 5/5 slab, the valence band widths (VBW) of Si- and SiC-derived bulk states compare fairly well for frozen and free surfaces, although they underestimate the respective bulk calculations (Table V). Increasing the slab thickness to 7/7 leads to VBW variations of only $\simeq 3\%$. We were able to estimate an error due to the slab approximation of ± 0.3 eV on LDA eigenvalues. A 7/7 slab is then large enough to get a good description of both the Si and SiC part, and the perturbation induced on the electronic structure by the interface configuration. In Fig. 7, the spatially projected Density Of States (DOS) at the interface is compared with the DOS obtained in inner layers at the Si and SiC sides of the slab. Several states lay in the band gap of the heterostructure, as obtained by alignment of the respective bulk valence bands (see Table V and the peak above the valence band top at Γ , highlighted by the arrow in Fig. 7). The Highest Occupied (HO) and Lowest Unoccupied (LU) states are located at 0.7 and 1.1 eV above the valence band top at Γ . These two states are also localized in the core of the edge dislocations, as a result of the large difference in charge transfer between Si-C and Si-Si bonds. In Fig. 8, the charge density plot of the HO state along the two dislocations directions is represented. The charge density is mainly localized on atoms of the $[1\bar{1}0]$ core dislocation, while no density is observed around the other core in the perpendicular direction. The opposite situation is found in other bonding states localized in the system forbidden gap and in particular for the LU state (see Fig. 9) whose charge density pertains to the dislocation core laying along the $[110]$ direction. Clearly, these states are true interface states, resulting from the reconstructed dislocation cores. It is worth noting that they would not be obtained from a coherent interface calculation, and that the determination of the electronic structure requires the atomic characterization of the misfit dislocation network.

It has been recently pointed out that a peak is observed in EELS and XPS around 0.8 eV.²⁹ Our results on the presence of interface states in the heterostructure forbidden gap may give an explanation for this experimental evidence.

VII. CONCLUSION

In conclusion, we have characterized the energetics, the atomic and electronic structure of the SiC/Si(001) interface. We performed first principles DFT-LDA, classical potential and elasticity theory calculations. The most stable atomic configuration is in agreement with experiments^{7,8,9}, where an array of misfit dislocations pinned at the interface is observed. Actually, from our

results, we also predict that the dislocation core is characterized by a substoichiometry in carbon atoms. Additional experiments are needed to confirm our proposed configuration: our relaxed structures may be used as input for simulating HREM experimental images and complement the results.

We furthermore estimated the interface energy from ab initio calculations, for a non-coherent interface, in the case of a multicomponent system, like SiC: this quantity, which is hardly accessible from experiment, has been here evaluated for the SiC/Si(001) interface, although with a non-negligible uncertainty. This is to our knowledge the first ab initio determination of interface energies at a mismatched semiconductor heterostructure.

Several electronic interface states, calculated at Γ , have been identified. These states, located on the core of the misfit dislocations, may influence the electronic and optical properties of the interface.

We point out that the approach we used in this study, *i.e.* the combination of elasticity theory, classical potential, and ab initio methods, may be easily adapted for other systems of interest, in particular for systems with large mismatch, where a coherent interface model is not suited, or for semiconducting systems, where core reconstructions are expected.

Acknowledgments

The authors want to thank Alexis Baratoff, Pierre Beauchamp and Matthieu George for fruitful discussions. One of us (LP) acknowledges INFM support for his stay in Italy as visiting professor. GC acknowledges Demichelis Foundation for financial support. Calculations have been performed in CINECA (Bologna, I) through the INFM Parallel Computing Initiative, at CSCS (Manno, CH), and at IDRIS (Orsay, F). This work was partially supported by INFM-PRA:1MESS.

-
- * Electronic address: Laurent.Pizzagalli@univ-poitiers.fr
- ¹ J. Dunstan, J. Mater. Sci.: Materials in Electronic **8**, 337 (1997).
 - ² S. C. Jain, A. H. Harker, and R. A. Cowley, Phil. Mag. A **75**, 1461 (1997).
 - ³ J. C. Bean, Proc. IEEE **80**, 571 (1992).
 - ⁴ J. Hoekstra and M. Kohyama, Phys. Rev. B **57**, 2334 (1998).
 - ⁵ R. Benedek, D. N. Seidman, and C. Woodward, J. Phys.: Condens. Matter **14**, 2877 (2002).
 - ⁶ S. R. Nutt, D. J. Smith, H. J. Kim, and R. F. Davis, Appl. Phys. Lett. **50**, 203 (1987).
 - ⁷ Q. Wahab, M. R. Sardela, Jr, L. Hultman, A. Henry, M. Willander, E. Janzén, and J.-E. Sundgren, Appl. Phys. Lett. **65**, 725 (1994).
 - ⁸ C. Long, S. A. Ustin, and W. Ho, J. Appl. Phys. **86**, 2509 (1999).
 - ⁹ M. Kitabatake, Thin Solid Films **369**, 257 (2000).
 - ¹⁰ V. Chirita, L. Hultman, and L. R. Wallenberg, Thin Solid Films **294**, 47 (1997).
 - ¹¹ J. Tersoff, Phys. Rev. B **39**, 5566 (1989).
 - ¹² G. Cicero, L. Pizzagalli, and A. Catellani, Phys. Rev. Lett. **89**, 156101 (2002).
 - ¹³ M. E. Levinshtein, S. L. Rumyantsev, and M. S. Shur, Editors, *Properties of Advanced Semiconductor Materials: GaN, AlN, InN, BN, SiC, and SiGe*, John Wiley and Sons, ISBN 0-471-35827-4, New York (2001).
 - ¹⁴ The elastic energy per unit area stored in the epilayers due to homogeneous strain is $E = 2\mu \left(\frac{1+\nu}{1-\nu}\right) h f_m^2$.² Taking average values for the shear modulus of elasticity μ and the Poisson's ratio ν , and given that the misfit f_m is 0.2 and a single SiC layer height h is 1.0875 Å, we obtained $E \approx 1.6 \text{ J/m}^2/\text{layer}$.
 - ¹⁵ F. Gao, E. J. Bylaska, W. J. Weber, and L. R. Corrales, Nucl. Instr. and Meth. in Phys. Res. B **180**, 286 (2001).
 - ¹⁶ We used the first principles molecular dynamics programs BASIC96 and JEEP (G. Galli and F. Gygi). For a review see, e.g., G. Galli and A. Pasquarello, in *Computer Simulation in Chemical Physics*, Edited by M.P.Allen and D.J.Tildesley, p. 261, Kluwer, Dordrecht (1993); and M. C. Payne, M. P. Teter, D. C. Allan, T. A. Arias, and J. D. Joannopoulos, Rev. Mod. Phys. **64**, 1045 (1993).
 - ¹⁷ W. Kohn and L. Sham, Phys. Rev. A **140**, 1133 (1965).
 - ¹⁸ D. Hamann, Phys. Rev. B **40**, 2980 (1989).
 - ¹⁹ G.-X. Qian, R. M. Martin, and D. J. Chadi, Phys. Rev. B **38**, 7649 (1988).
 - ²⁰ V. Fiorentini and M. Methfessel, J. Phys.: Condens. Matter **8**, 6525 (1996).
 - ²¹ Note that these values are very slightly different from those given in the reference¹², due to a small energy gain obtained from a recent improvement in the relaxation of the S1a configuration.
 - ²² H. Balamane, T. Halicioglu, and W. A. Tiller, Phys. Rev. B **46**, 2250 (1992).
 - ²³ C. Sbraccia, P. L. Silvestrelli, and F. Ancilotto, Surf. Sci. **516**, 147 (2002).
 - ²⁴ G. Xu and Z. Feng, Phys. Rev. Lett. **84**, 1926 (2000).
 - ²⁵ R. Bonnet and J. L. Verger-Gaugry, Phil. Mag. A **66**, 849 (1992).
 - ²⁶ J. P. Hirth and J. Lothe, *Theory of dislocations* (Wiley, 1982).
 - ²⁷ A. Plöbl and G. Kräuter, Mater. Sci. Eng. R **25**, 1 (1999).
 - ²⁸ J. E. Northrup, Phys. Rev. B **44**, 1419 (1991).
 - ²⁹ U. del Pennino and M. De Crescenzi, private communication.

Table captions

TABLE I: Optimized chemical potentials and lattice constants for Si and 3C-SiC bulks, computed with the Tersoff potential and the ab initio method. For ab initio, the bulk calculations (column "*bulk*") and the value obtained from linear extrapolation²⁰ (column "*lin*") are indicated for comparison.

TABLE II: Configuration energy differences, from classical dynamics, and variation of C and Si atoms, for the first set of configurations and a 12/8 system (see Fig. 1), with the geometry S1a taken as the reference.

TABLE III: Configuration energy differences for CSS compared to S1a, within different conditions, and slab size. As indicated in the text, numbers for the classical simulations are slightly different from those reported in Ref.¹², because of improved convergence. The ab initio values are obtained with the linear extrapolation method²⁰, and the consistently derived chemical potentials were used.

TABLE IV: Surface energies for the systems used in the slab calculations, computed with the ab initio method. The pseudo-hydrogen energy is included, as detailed in the text.

TABLE V: Valence band Width (VBW) and energy gap (Δ_{gap}) of the relaxed structures in eV.

	Tersoff		Ab initio		
	μ_0 (eV)	a_0 (Å)	μ_0 (bulk) (Ha)	μ_0 (lin) (Ha)	a_0 (Å)
Si	-4.630	5.432	-3.96611	-3.96877	5.401
SiC	-12.374	4.318	-9.64469	-9.65374	4.334

Table I

Config.	Δn^{Si}	Δn^{C}	ΔE_α (eV/cell)	
			C-rich	C-poor
S1a	0	0	0.0	0.0
S1b	0	0	6.55	6.55
P1	0	-9	16.40	9.92
P2	-9	-9	40.09	40.09
S2	0	0	37.91	37.91
C2	-25	16	63.74	93.26
C1	-25	25	63.88	99.88

Table II

ΔE_α	Tersoff		Ab initio	
(eV/cell)	12/8	36/36	5/5	7/7
C-rich	-6.04	-6.03	-5.90	-5.69
C-poor	-15.40	-15.39	-15.26	-15.05

Table III

E_S (Ha/at-H ₂)	C-rich	C-poor
Si(001)-(1x1)	-1.12208	
C:SiC(001)-(1x1)	-1.14212	-1.12890

Table IV

System	VBW (eV)			$\Delta_{gap}(eV)$
	SiC	Si	Total	
Si bulk	-	12.08	-	-
SiC bulk	15.68	-	-	-
5/5 frozen surf.	14.67	10.91	15.31	0.50
5/5 free surf.	14.65	9.95	14.68	0.96
7/7 frozen surf.	15.06	11.25	15.57	0.40

Table V

Figure captions

FIG. 1: First set of initial configurations. White (black) circles represent the Si (C) atoms. The dashed line shows the location of the interface.

FIG. 2: $[110]$ (left) and $[1\bar{1}0]$ (right) side views of three relaxed SiC/Si(001) interface configurations. Light grey (black) spheres show silicon (carbon) atoms. The dashed thick lines mark the location of the extra atomic planes introduced by the misfit edge dislocations. Note that the represented bonds are drawn solely on the basis of a distance criterion and are not necessarily indicative of a true chemical bond. Removal of the C atoms inside the ellipses leads to the CSS configuration.

FIG. 3: $[110]$ (top) and $[1\bar{1}0]$ (bottom) perspective side views of the most stable CSS SiC/Si(001) interface configuration. Light grey (black) spheres show silicon (carbon) atoms.

FIG. 4: Layer warping for a $7/7$ SiC/Si(001) interface. In abscissa, the mean value of the coordinate normal to the interface plane for a given atomic layer is indicated.

FIG. 5: Contour plot of the strain field at the $7/7$ SiC/Si(001) interface projected along the $[1\bar{1}0]$ direction for both the CSS (top) and S1a (bottom) geometries, evaluated in terms of atomic displacements from ideal bulk-like positions. To enhance comparison, the displacement integrated over a supercell plane of fixed height from the interface is indicated. Two lateral replicas are indicated for both configurations, with the SiC part higher and Si lower; brighter regions depict larger distortions: they occur slightly below the interface, at the Si first layer.

FIG. 6: Interaction energy between surface and interface as a function of the slab size, for the S1a (left) and CSS (right) configurations.

FIG. 7: Calculated DOS for the CSS configuration and a $7/7$ slab, projected on the Si and SiC layers at the interface (top panel), compared with the DOS for bulk SiC and Si (middle and bottom panels). The width of Si and SiC bands, as well as the energies of HO and LU states, are shown in the figure.

FIG. 8: Isosurface (medium grey) of the highest occupied state projected along $[110]$ (left) and $[1\bar{1}0]$ (right). Black (light grey) spheres indicate C (Si) species. Surface atoms are saturated with hydrogens (small white spheres).

FIG. 9: Isosurface (medium grey) of the lowest unoccupied state projected along $[110]$ (left) and $[1\bar{1}0]$ (right). Black (light grey) spheres indicate C (Si) species. Surface atoms are saturated with hydrogens (small white spheres).

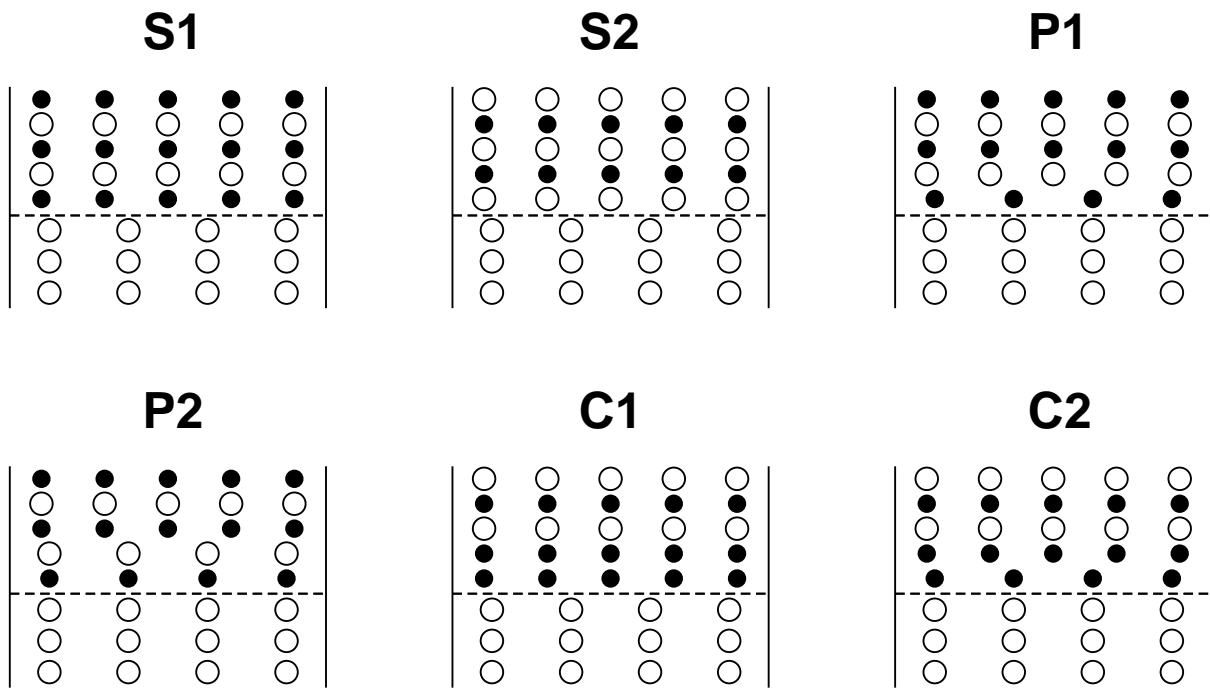


Figure 1

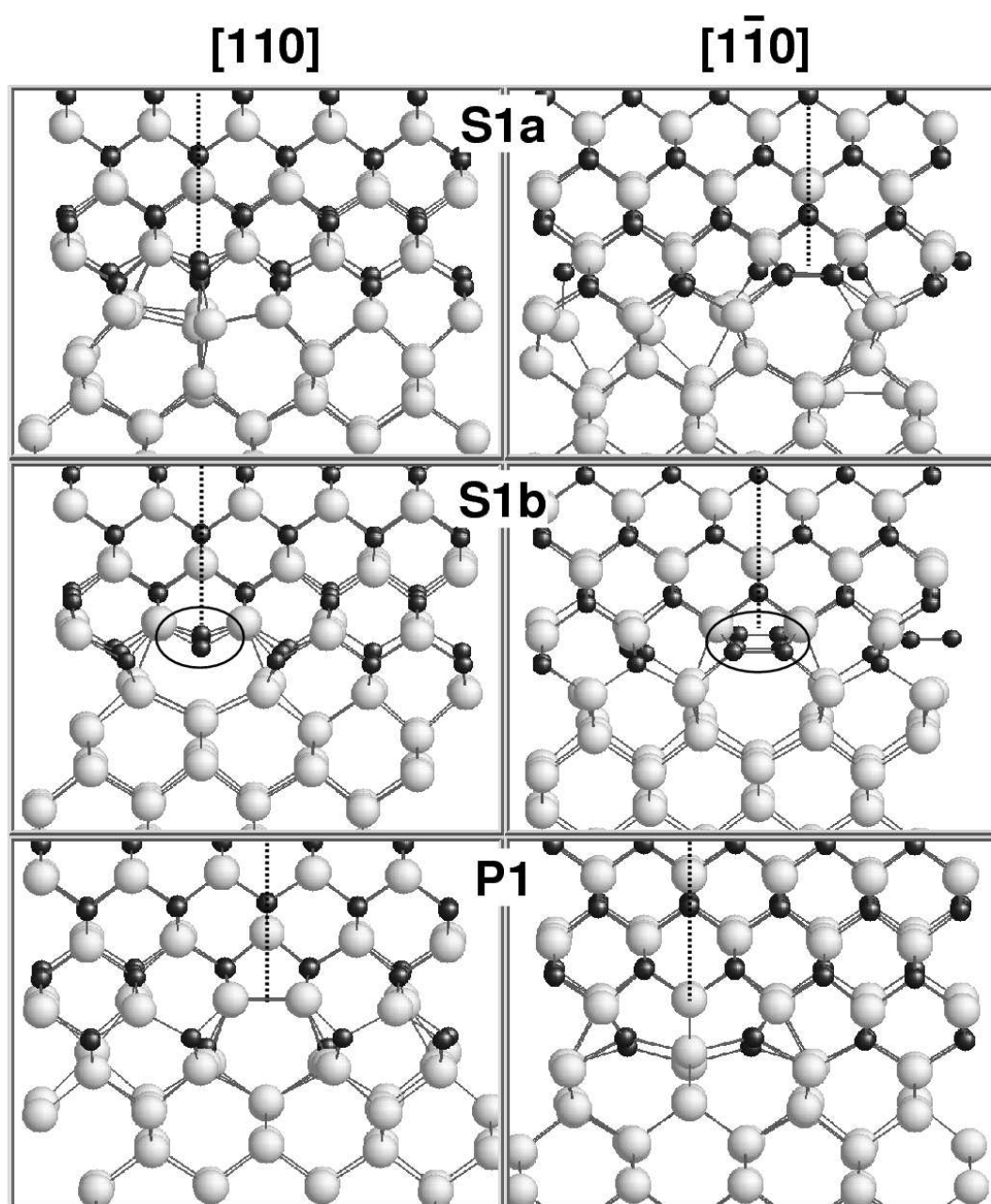


Figure 2

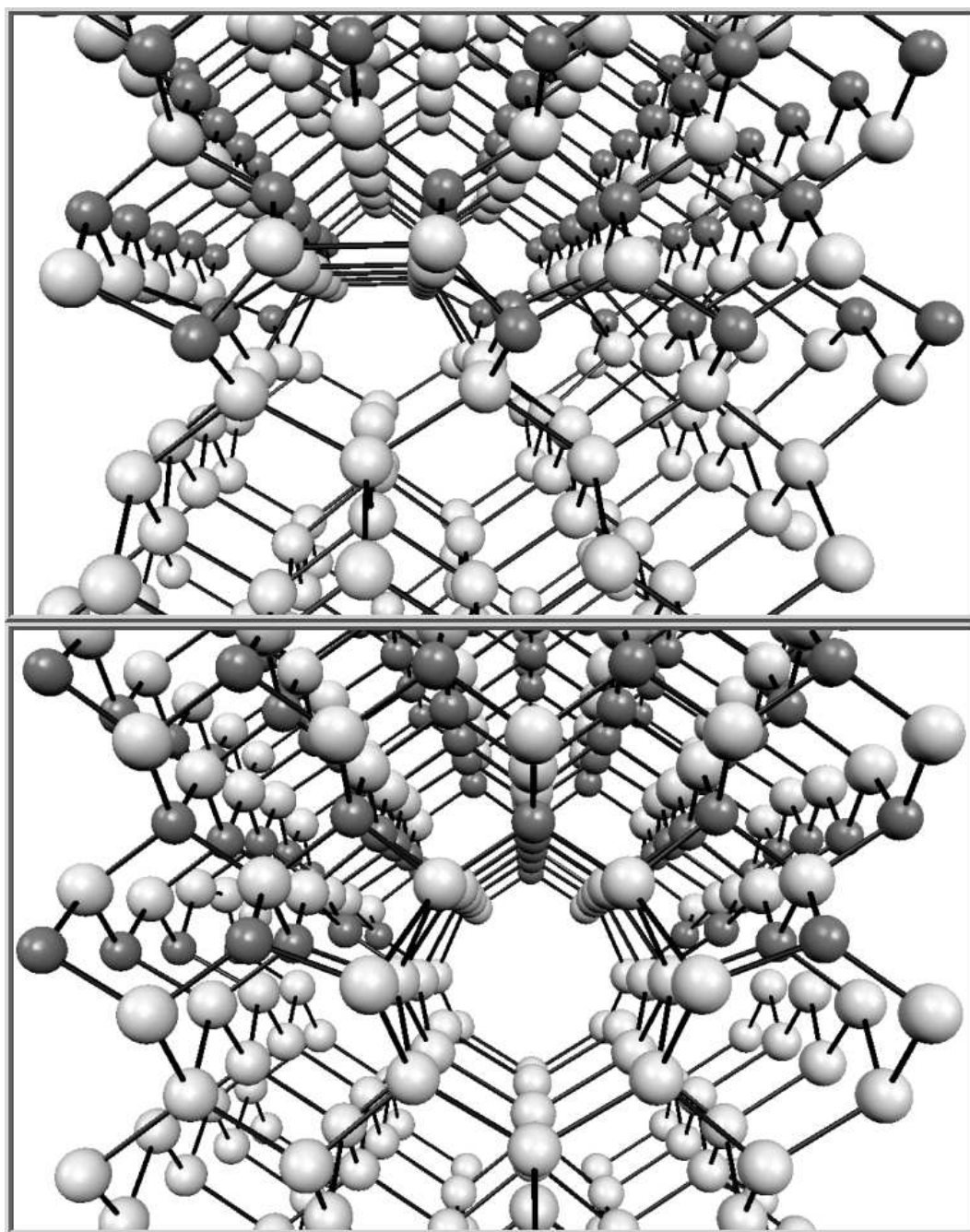


Figure 3

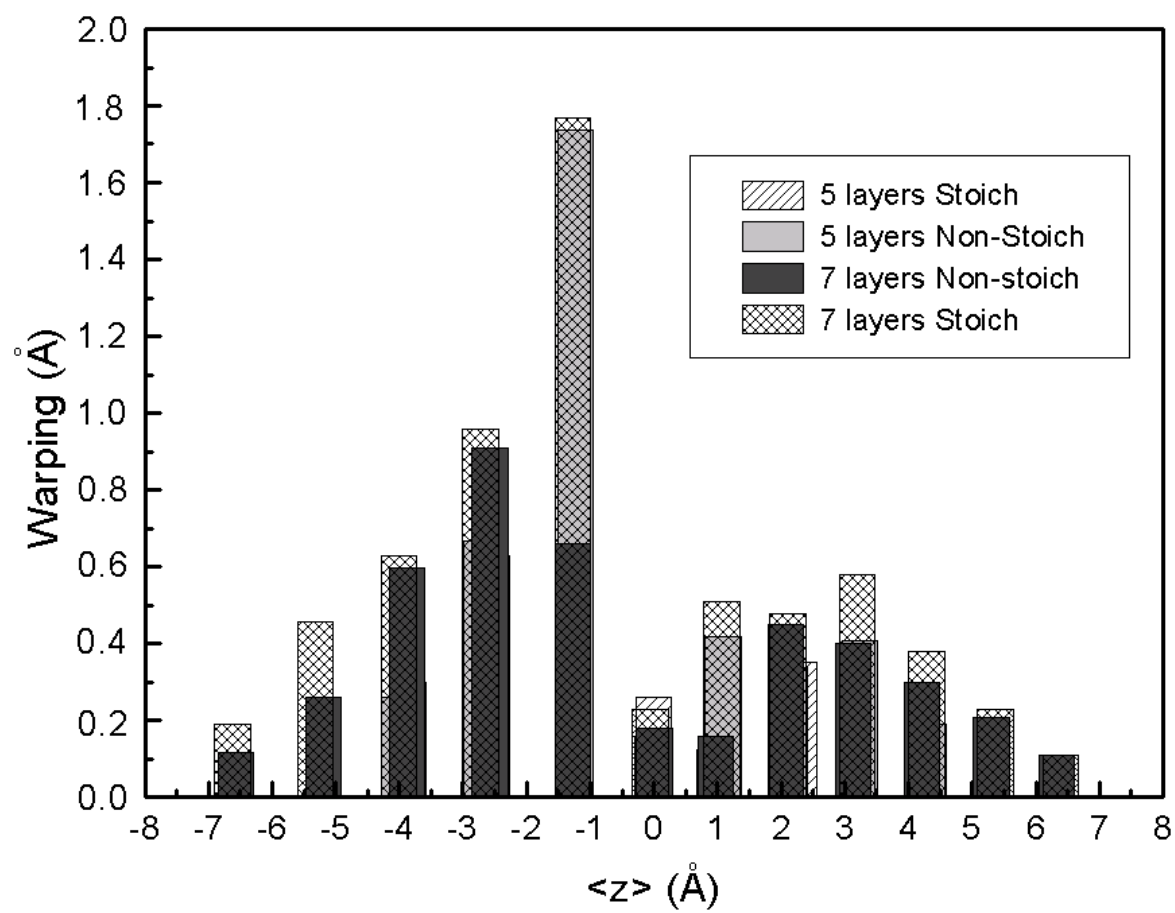


Figure 4

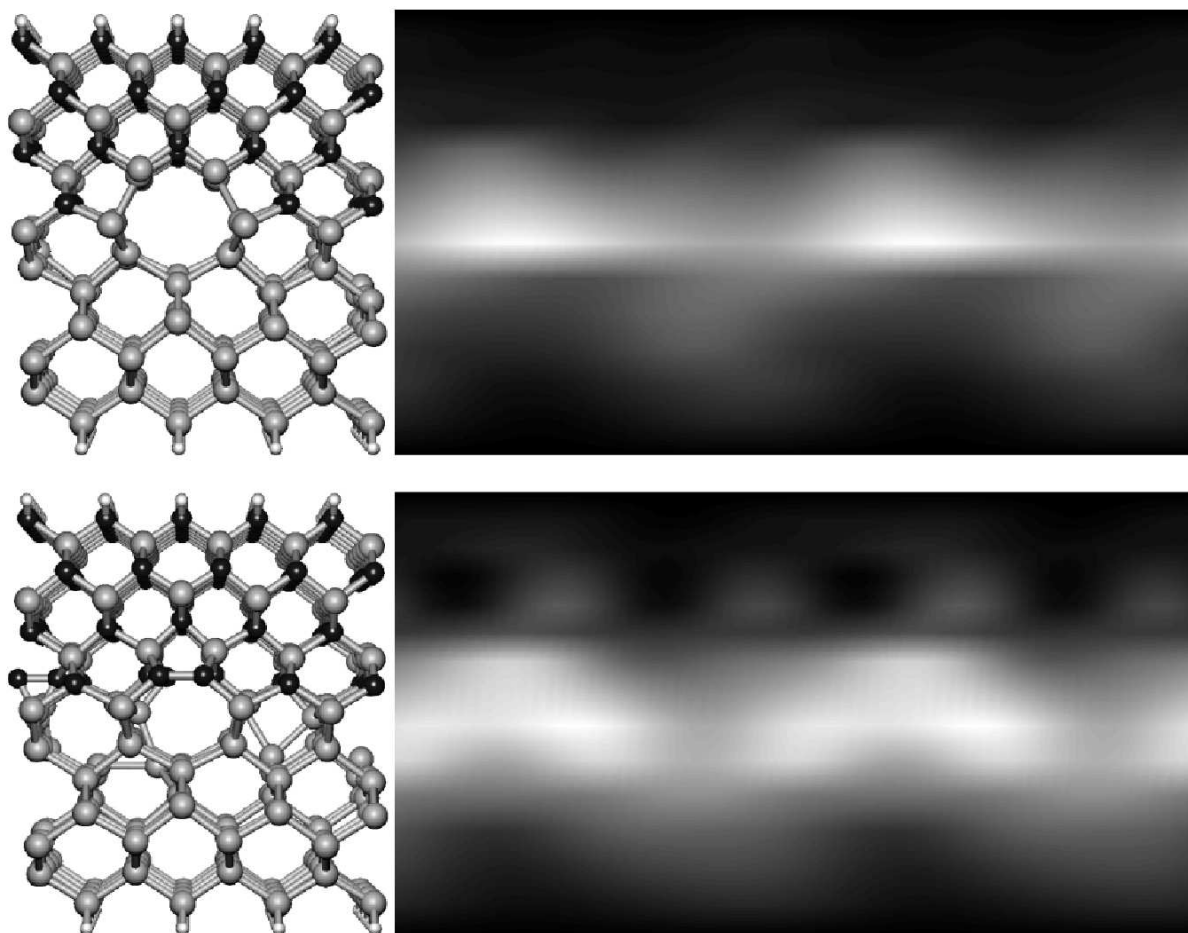


Figure 5

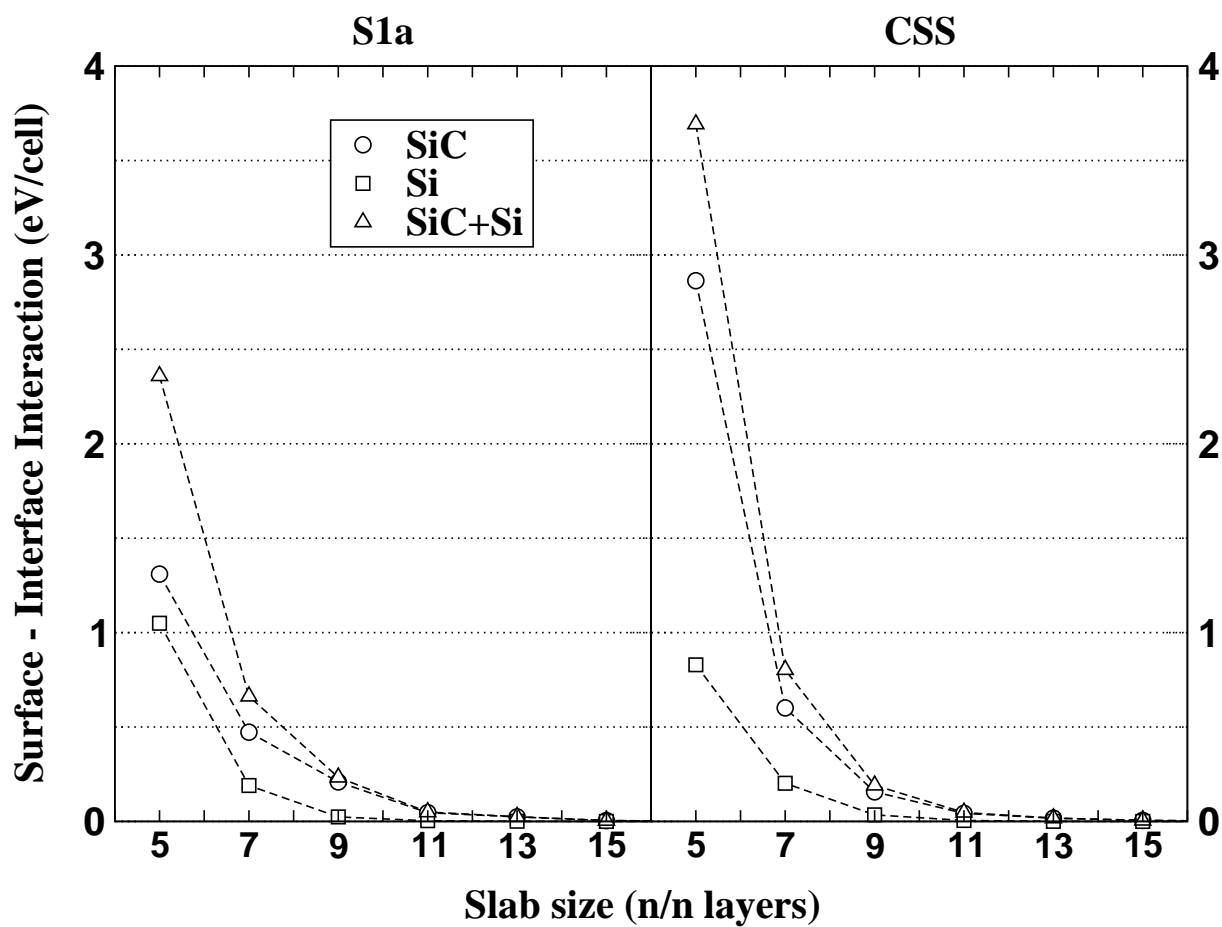


Figure 6

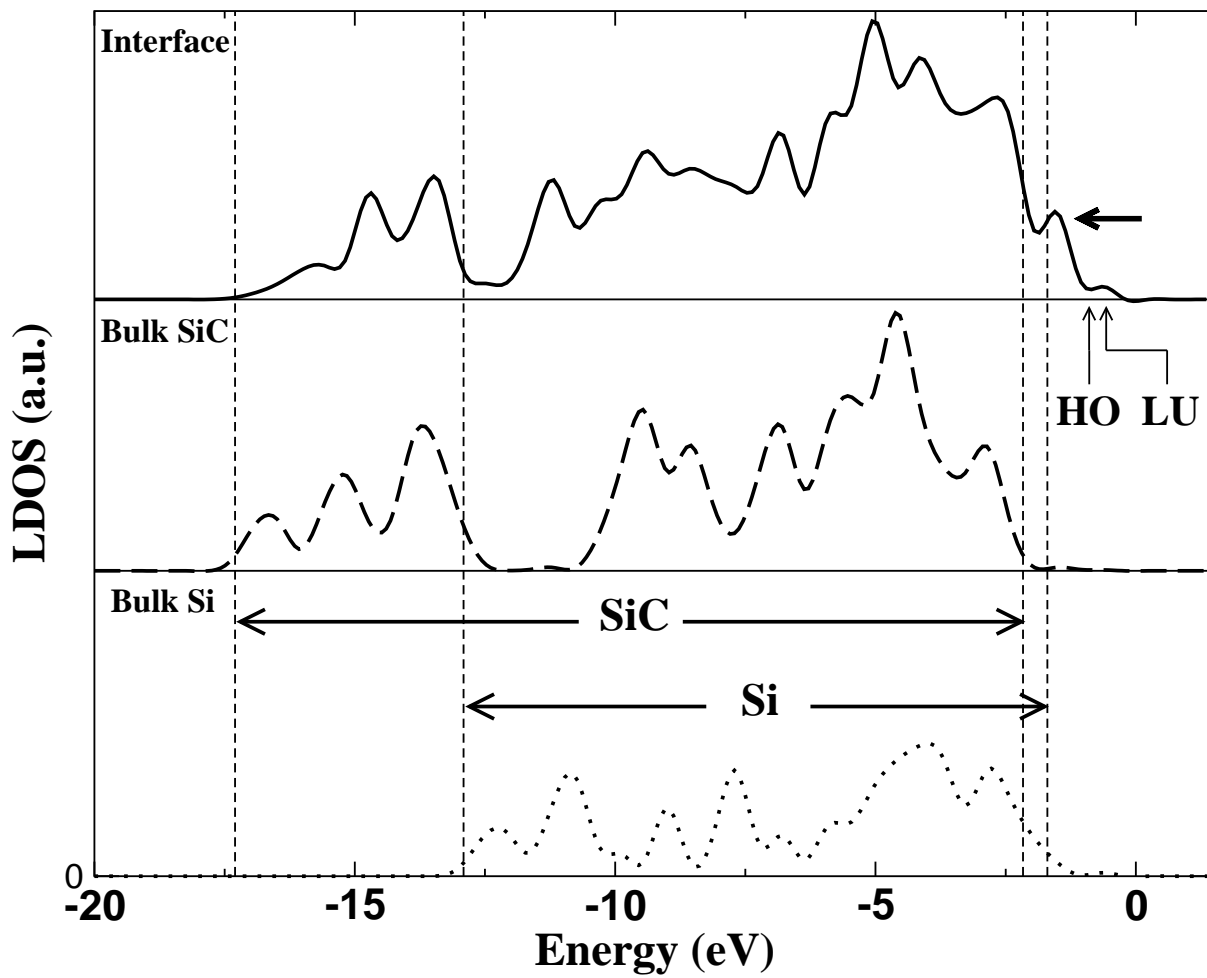


Figure 7

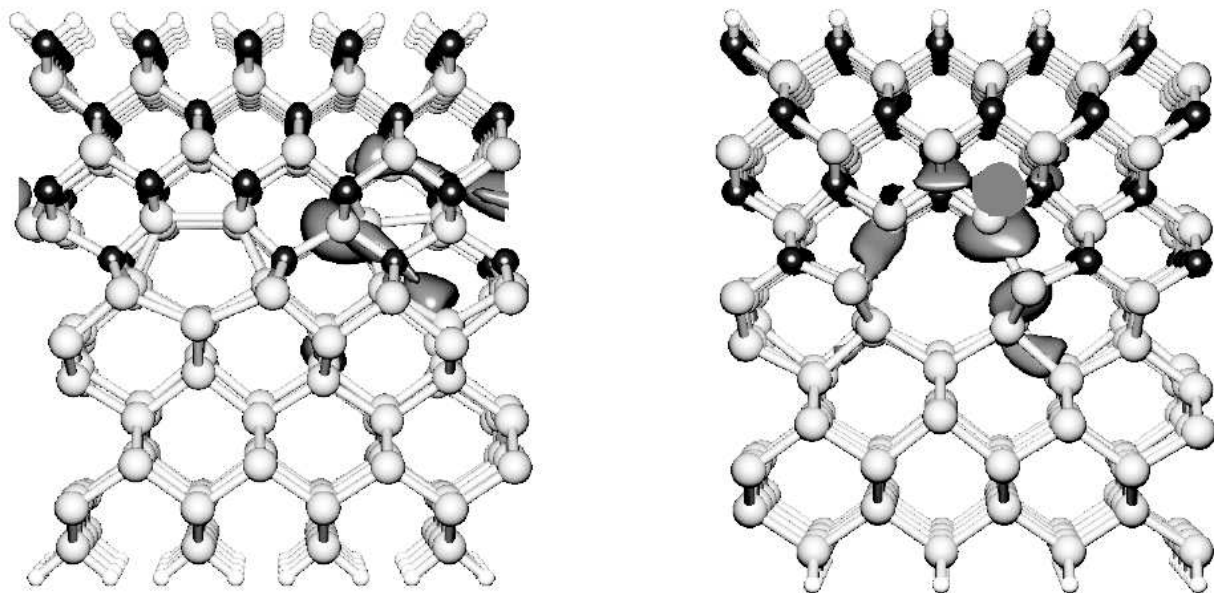


Figure 8

Figure 9

